DOI: 10.61782/fa.2025.0191

FORUM ACUSTICUM EURONOISE 2025

CHARACTERISATION AND CONTROL OF AERO-ACOUSTICAL INFLOW NOISE SOURCES OF THE EVAPORATOR FAN IN HEAT PUMPS

Frieder Lörcher* **Sandra Hub**

ZIEHL-ABEGG SE, 74653 Künzelsau, Germany

ABSTRACT

Recent heat pump fans are nowadays often optimized towards a very low self-noise level. Still less effort is expended in the field of additional noise sources generated by spatially and temporally inhomogeneous inflow to the fan, in particular the tonal unsteady loading noise and the broadband turbulence ingestion noise, which depend mainly on the upstream installation conditions and are therefore called “inflow noise”. It is shown for a state-of-the art air-to-water heat pump with 12 kW rated capacity and an evaporator heat exchanger in L-form that the inflow noise exceeds the self-noise of the fan given by the fan supplier. The conclusion is that the optimisation potential considering the inflow noise is more promising than considering a further self-noise optimisation of the fan.
For the considered device, the inflow noise is analysed and characterized along with the causal inhomogeneous inflow conditions to the fan. Both numerical and experimental results are presented. Some optimizing approaches to reduce the inflow noise are investigated, considering both the fan design and installation arrangement. The A-rated total noise emission can be reduced, but, more important, the annoying tonal character of the noise can be attenuated significantly.

Keywords: *heat-pumps, fans, fan-noise, installation noise, aeroacoustics, tonality*

*__Corresponding author__: frieder.loercher@ziehl-abegg.de

1. INTRODUCTION

Heat pumps have become established as efficient and environmentally friendly solutions for the heating and cooling of buildings. Despite their numerous advantages, the noise emitted by the outdoor units (evaporators) poses a significant challenge - particularly in residential areas where low sound levels are required. A substantial proportion of this noise arises from aeroacoustic phenomena associated with the operation of the evaporator fans.
The analysis and control of these noise sources are essential for improving acoustic comfort and enhancing the acceptance of heat pump systems. In recent years, fan researchers and manufacturers have made considerable progress in reducing the sound power levels of their products. However, the focus of such development work is often limited to the fan's intrinsic noise under laboratory conditions, as for example the tip gap noise [2] or stall-related noise [3]. When integrated into actual heat pump systems, significantly higher noise levels are frequently observed. Installation effects of fans in heat pumps concerning efficiency have been investigated in [4]. In [5], the installation fan noise induced by upstream located heat exchangers is investigated.
This study focuses on the mechanisms responsible for the additional aeroacoustic noise (installation noise) generated by evaporator fans in heat pumps, which go beyond the fan's self-noise. These mechanisms are categorised into two principal types: tonal and broadband installation noise. Based on numerical simulations and experimental measurements carried out on a specific evaporator configuration from the publicly funded collaborative "WarmHome" project [1], models for these noise sources are presented, along with strategies for their mitigation.

2. EVAPORATOR AND REFERENCE FAN IN THE WARMHOME PROJECT

In the WarmHome project, a specifically designed L-shaped evaporator heat exchanger with dimensions Width x Depth x Height = 1070 mm x 315 mm x 1200 mm is used to enable particularly compact integration into the heat pump's installation space. The L-shaped geometry induces a deflection of the airflow within the outdoor unit, resulting in more inhomogeneous inflow conditions at the evaporator fan. These installation-specific conditions form the basis for the aeroacoustic effects investigated in this study. A sample of the heat exchanger mounted in a wooden mock-up of the airside of the evaporator is shown in Figure 1.

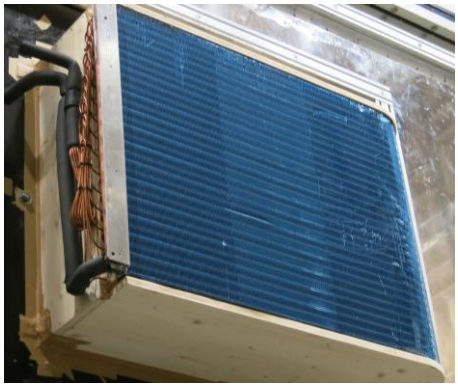

Figure 1. The L-shaped evaporator heat exchanger mounted in the test chamber.

To investigate the relevant noise generation mechanisms and possible optimization approaches, a reference fan was selected that reflects the current state of the art. The chosen axial fan is the commercial fan ZIEHL-ABEGG FPowlet [6] with rotor diameter of 630 mm, 3 impeller blades and a maximum rotation speed of 770 rpm. It is suitable for an operating point of 5000 m³/h at 17 Pa at rotation speed 475 rpm and features low self-noise emission levels. The total sound power of the self-noise given in the data sheet at the nominal operating point is 49 dB(A). This makes it a suitable match for the air-to-water heat pump with a heating capacity of 12 kW to be developed within the project, using the selected evaporator heat exchanger. A model of the fan is shown in Figure 2. The with aerodynamic parts are made of glass fibre reinforced polypropylene

The combination of the L-shaped heat exchanger and the reference fan represents the system under acoustic investigation. This system and variations of it were analysed both experimentally under controlled conditions in a free-field environment and numerically using Lattice-Boltzmann simulation methods.

Figure 2. Reference fan FP063.

3. EXPERIMENTAL SETUP

Aeroacoustic experiments are performed in the ZIEHL-ABEGG anechoic facility with experimental fan testing according to ISO 5801 [7]. The test rig consists of two large anechoic rooms separated by a partition wall. The fan or evaporator unit were attached und integrated with in the partition wall between an upstream and a downstream plenum. Both the inlet plenum (Figure 3) and the outlet plenum have non-reflective walls down to 100 Hz and have dimensions of 9 m x 9 m x 9 m.. Using this experimental setup, the baseline evaporator configuration, the baseline fan and variations thereof are analysed. The volume flow rate Q_V, the static pressure rise Δp_{stat} between the plenums and the shaft input power P_1 are recorded for different duty points, as well as the A-rated specific sound power levels L_W5 and L_W6 on the suction and pressure side, respectively, with the hull surface method. To obtain the total sound power level, the two sound power levels can be summed up using the logarithmic summation rules for level quantities.

Figure 3. Inlet plenum of the anechoic test facility with fan mounted in separation wall.

In addition to the sound power levels, a narrow band spectral decomposition of the emitted sound can be

obtained using the recorded sound signals of the 2 x 12 microphones used for sound analysis.

4. NUMERICAL METHOD

4.1 Numerical Setup

For deeper insight to flow phenomena, numerical simulations using the commercial PowerFLOWsolver 5.5a based on the Lattice-Boltzmann Method (LBM) are performed. The LBM is naturally transient and compressible providing a direct insight into hydrodynamic mechanisms responsible for the acoustic sources but also into acoustic propagation. The LBM tracks the time and space evolution of a truncated particle distribution function on a lattice grid. The particle distribution evolution is driven to the equilibrium by the so-called collision operator. The discrete Lattice-Boltzmann equations are solved with 19 discrete velocities for the third order truncation of the particle distribution function, which has been shown sufficient to recover the compressible Navier-Stokes equations for a perfect gas at low Mach number in isothermal conditions [8]. In PowerFLOW, a single relaxation time is used, which is related to the dimensionless laminar kinematic viscosity [9]. This relaxation time is replaced by an effective turbulent relaxation time that is derived from a systematic Renormalization Group procedure detailed in [10]. It captures the large structures in the anechoic room but also the small turbulent scales that develop along the wall surfaces in a Large Eddy Simulation manner. The particular extension developed for rotating machines can be found in Pérot et al. [11]. The computational domain includes the two coupled anechoic rooms as shown in Figure 4.

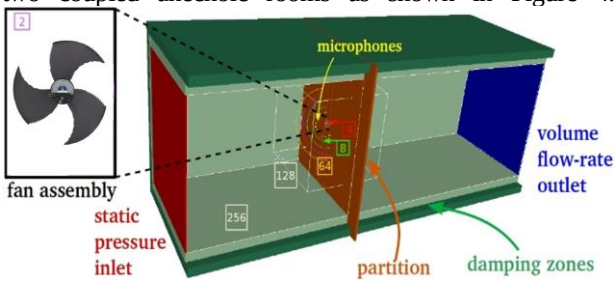

Figure 4. Computational domain and refinement volume definitions. Numbers in squares provide the mesh size in mm for the outlined refinement

The square cross section of the simulation volume has a width of 10 m and the upstream and downstream plenums are also 30 m and 20 m long, respectively. The atmospheric pressure p = 101325 Pa is imposed on the left red surface, while the volume flowrate Qv is imposed on the downstream blue surface. The convergent inlet nozzle and detailed geometry of the fan impeller are considered. Only the motor and its shaft are discarded in the numerical setup. The mesh resolution in the domain is defined through successive embedded volumes, outlined in Figure 4, the mesh size being decreased by a factor of 2 between them. The resolution around the fan blades and the inlet nozzle wall is 0.5 mm. The volume around the fan is defined as a rotating volume at a rotational speed. Extended logarithmic wall functions to account for adverse and favourable pressure gradients [12] are applied on all wall surfaces. The total numerical domain counts 98 million cells and 7 million surface elements. Simulations are performed for several flow rates. First, the setup is initialized in two steps from pre-converged flow obtained from simulations with coarser meshes without the highest resolved refinement regions (50 revolutions computed on the mesh with maximum resolution of 2 mm and subsequently, 25 revolutions computed on the mesh with maximum resolution of 1 mm). Then, the finest mesh is used for performance prediction. The convergence is obtained after 2 fan revolutions on the finest mesh, and data are acquired for 5 fan revolutions. Static pressure is recorded at the exact locations of the microphones in the experiments. In addition, some cross-sections including the one at mid-blade height (midspan) and blade surface are recorded at high frequency sampling for frequency analysis.

4.2 Ingestion Turbulence Modelling

The modelling of the turbulence generated by the heat exchanger is crucial to get a good prediction of the installation noise for the installed condition. Three variants have been considered: Treatment of the heat exchanger as porous block; the same with modelled cooling liquid tubes downstream of the porous block and the use of a turbulent seeding with data obtained from a highly resolved simulation of a small heat exchanger segment. The latter is quite complex, and as the version with the modelled tubes gave similar results, it was applied for the present study.

4.3 Quality of numerical results

The numerical model presented above is validated through the comparison of performances with experimental measurements acquired on the certified ISO 5801 ZIEHL-ABEGG facilities. In Figure 7, a simulated sound power spectra comparison of the fan alone and the fan in installation situation is shown. The results must be seen in

comparison with the experimentally measured ones in Figure 6. At least the trend between the two, and thus the installation sound, is captured well by the simulations.

5. CHARACTERISATION OF INSTALLATION NOISE

5.1 Decomposition to Self-Noise and Installation Noise

The overall sound level of an evaporator fan in a heat pump primarily consists of two components: the self-noise of the fan and the installation noise, which arises from the specific integration of the fan into the device. Additional aerodynamic noise sources may also contribute, such as protective grille noise, but these are not considered in this study. Installation noise can be calculated as the difference between the total sound level in the installed condition and the isolated self-noise of the fan, typically determined under laboratory conditions. This approach applies to both overall sound power levels and their spectral representation.

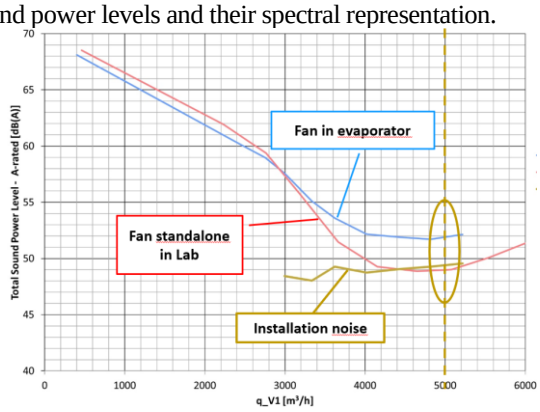

Figure 5. Decomposition of the fan noise in the evaporator installation condition

Figure 5 shows A-weighted overall sound power levels based on experimental measurements of the standalone fan and the fan installed within the evaporator for constant rotation speed and varying airflow Q_V (varying device resistance). The figure also includes the computed difference between both conditions (note that the subtraction must be performed using de-logarithmised sound power values). This difference is referred to as the inflow noise component associated with the heat exchanger measurement. It reaches a magnitude comparable to the fan's self-noise. At the highlighted operating point—corresponding to the nominal design point of the heat pump of Q_V=5000 m³/h—the installation noise component is even slightly higher than the fan's self-noise.

In typical heat pump applications, installation noise can significantly exceed the fan's self-noise—especially when an already acoustically optimised fan is used, as the optimisation typically focuses on the fan's self-noise emission. Consequently, the targeted reduction of installation noise represents a particularly promising strategy and an important measure for improving the overall acoustic performance of the system.

5.2 Spectral Analysis of Installation Noise and Tonality

The subtraction method for determining installation noise, as described in the previous section, can also be applied to sound power spectra, i.e. the frequency-resolved representation of sound power levels. Figure 6 shows a spectral comparison between the self-noise of the reference fan and the total noise measured in the installed configuration within the evaporator at the nominal operating point of Q_V= 5000 m³/h. The abscissa indicates the dimensionless frequency, expressed as multiples of the blade passing frequency (BPF), which is defined as the product of the number of blades and the rotational frequency of the impeller.

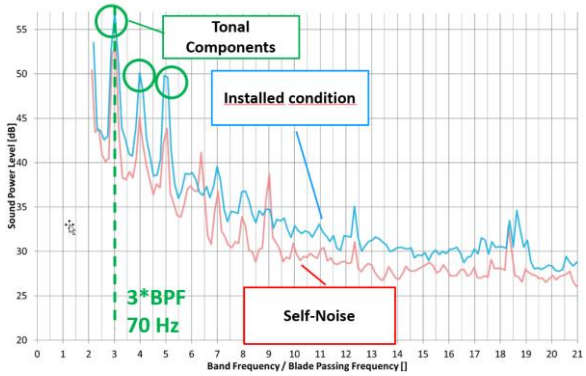

Figure 6. Total sound and self-noise (exp.)

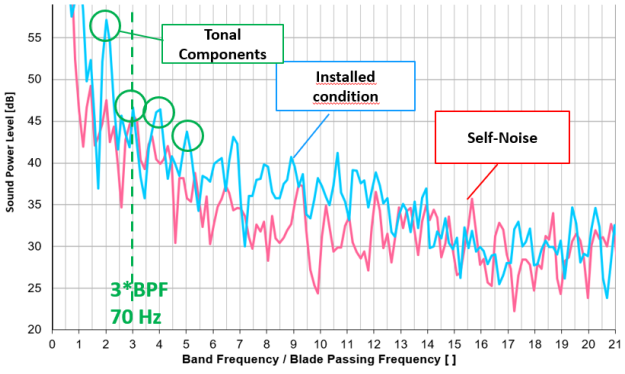

Figure 7. Total sound and self-noise (sim.)

The figure clearly reveals that tonal components are amplified at integer multiples of the BPF, and that the broadband noise level also increases in the installed condition. Figure 8 illustrates the resulting installation noise—i.e. the difference between total and self-noise—along with the self-noise spectrum for comparison. While both exhibit similar overall sound power levels, the installation noise in the current configuration shows a significantly more tonal character. This is a common observation in heat pump noise measurements, and it results in a perceptibly more tonal quality of the sound emission, as also evident in Figure 6.

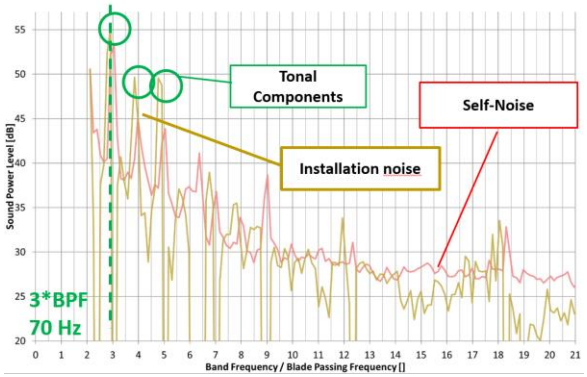

Figure 8. Spectral decomposition of installation noise and self-noise

Tonal sound components are generally perceived as more annoying. Therefore, standard [13] defines a concept of a tonality penalty, which adds a level adjustment in (dB) in cases where prominent tonal peaks occur in the noise spectrum. This approach is increasingly applied in the heat pump industry. According to Figure 6, the self-noise of the fan does not justify any tonality penalty, whereas the total noise measured in the installation condition results in a penalty of +2 dB. Consequently, from an acoustic design perspective, the tonal component of the installation noise should be a key area for system-level optimisation.

5.3 Generation Mechanisms

Installation noise can be divided into two main components:

- **Tonal components**, which appear as narrowband peaks in the frequency spectrum
- **Broadband components**, which manifest as a spectrally distributed sound power over a wide frequency range

These two types of noise result from distinct underlying physical mechanisms. A brief description of these is provided to better support the optimisation strategies discussed in later sections.

5.3.1 Generation Mechanisms of Tonal Installation Noise

Tonal noise components are typically caused by **unsteady aerodynamic loading**, which arises from time-averaged asymmetric inflow conditions. These may be induced by skewed or one-sided inflow, transitions from rectangular ducts, inflow grilles, bends, or obstructions in the intake region. Such features create a non-rotationally symmetric pressure field at the fan inlet, through which the rotor blades pass periodically. The resulting sound radiation occurs at discrete frequencies, often at multiples of the blade passing frequency (e.g. 3×BPF ≈ 70 Hz), and significantly contributes to the perceived tonality of the total sound.

5.3.2 Generation Mechanisms of Broadband Installation Noise

Broadband noise components primarily originate from the **interaction between the fan and turbulent structures** in the inflow, which are inherently unsteady and time-varying. Due to the stochastic distribution of their size, intensity, and form, the resulting sound has a broadband spectral character. These turbulent structures may arise from sharp flow deflections, abrupt geometry changes, structural elements such as struts, flow separations at the heat exchanger, or large stationary vortices.

The interaction with these turbulence-induced structures results in broadband pressure fluctuations at the blade surfaces, which are converted into acoustic emissions. The frequency content of this noise is related to the characteristic scale of the vortices—larger vortices generally lead to lower-frequency components. While this type of noise typically has less impact on the fan's aerodynamic performance, it can significantly contribute to the radiated sound power.

Notably, mechanisms that generate tonal noise—such as time-averaged inhomogeneous inflow fields—can also induce **secondary broadband noise components**, due to the additional generation of turbulence in the vicinity of the rotor.

6. OPTIMIZATION APPROACHES CONCERNING THE TONAL INSTALLATION NOISE

Three optimization approaches specifically aiming at the reduction of tonal installation noise by homogenising the inflow have been tested and are briefly described in this section.

6.1 Optimization of component arrangement

This is often the most cost-effective approach to reduce tonal—and potentially also broadband—installation noise, as it requires no additional components. Instead, the existing elements, particularly the fan, are arranged within the heat pump to achieve the most symmetrical inflow conditions possible at the fan inlet.
Figure 9 shows a visualisation of the time-averaged inflow velocity field—specifically, the circumferential velocity component VT—on a plane upstream of the fan impeller. The reference evaporator configuration, as analysed in Section 5, serves as the basis. A pronounced asymmetry in the inflow distribution can be observed, which is likely caused by the L-shaped geometry of the heat exchanger.

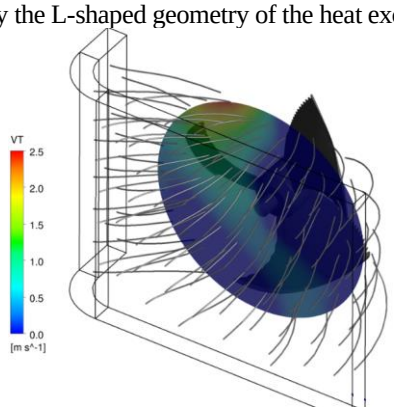

Figure 9. Time-averaged fan inflow velocity VT (reference configuration, simulation)

Shifting the fan approximately 10 cm towards the short branch of the L-shaped heat exchanger results in a more homogeneous inflow distribution, as shown in Figure 10.

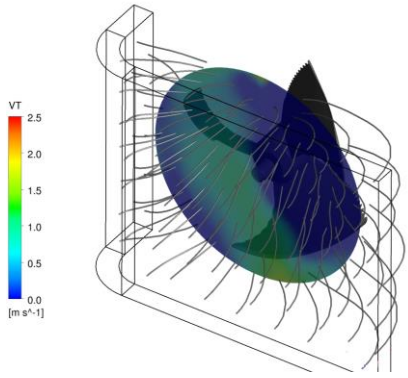

Figure 10. Time-averaged fan inflow velocity VT (optimized configuration, simulation)

The corresponding sound power spectrum, in comparison with the reference configuration, is presented in Figure 11. A substantial reduction in tonal components can be observed. According to [13], no tonal penalty is applicable in the optimised configuration—representing a significant acoustic improvement, even though the A-weighted total sound power level (not shown) remains nearly unchanged. In conclusion, careful spatial arrangement of components—particularly to achieve the most symmetrical and undisturbed fan inflow possible—proves highly effective in reducing the tonal content of heat pump noise emissions.

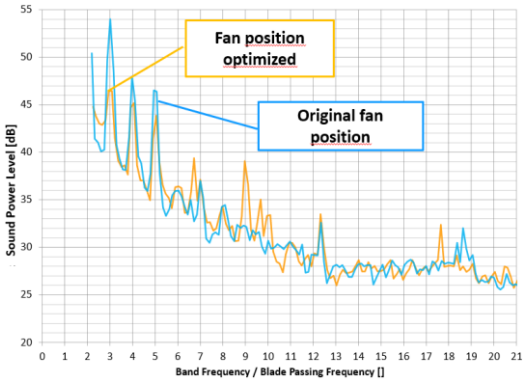

Figure 11. Spectral decomposition of the total noise (fan position optimization)

6.2 Use smooth flow-guiding wall elements

The flow-guiding elements depicted illustrated in Figure 12 were designed to reduce tonal noise by promoting a smoother and more symmetrical inflow distribution to the fan—primarily through the suppression of so-called corner vortices, potentially also reducing inflow turbulence and associated broadband noise. Previous investigations on a planar heat exchanger demonstrated that the implementation of four such elements, realised as 3D-printed parts and placed in each of the four corners, resulted in a significant reduction in installation noise tonality. In the present configuration, however, only a marginal improvement was achieved, and the tonal penalty could not be eliminated. This underlines that the effectiveness of such measures is highly case-specific. Therefore, the potential benefits of flow-conditioning elements should always be assessed through numerical simulations or prototype testing.

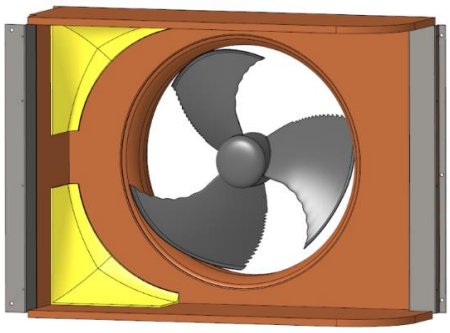

Figure 12. Flow-guiding wall elements (CAD, yellow)

6.3 Use of an inflow grid

To homogenise the inflow to the fan and reduce tonal as well as low-frequency broadband noise associated with large-scale vortical structures, inflow grids represent a promising solution. Figure 13 shows the CAD model of an inflow grid investigated in the present study.

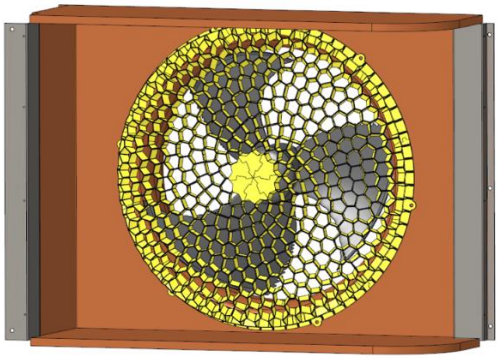

Figure 13. Inflow grid (CAD, yellow)

The corresponding comparison of the sound power spectra is shown in Figure 14. Similar to the optimised fan position (note: in this case, the fan position is not optimised), the tonal components are noticeably reduced, resulting in the elimination of the tonality penalty. In contrast to Figure 11, a broadband reduction in sound power is observed in the low-frequency range—likely due to the smoothing of large-scale vortical structures by the inflow grid. However, at higher frequencies, the installation noise increases, as the grid itself generates fine-scale turbulence. As a consequence, the A-weighted total sound power level is elevated when the inflow grid is used, making this approach less favourable than fan position optimisation in the present configuration.

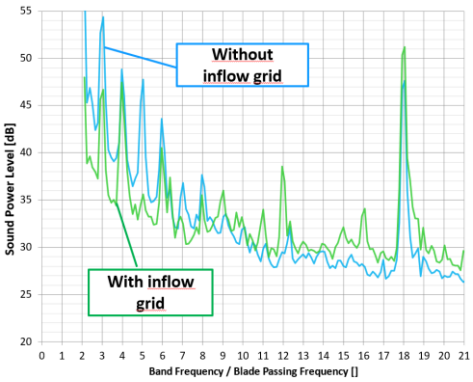

Figure 14. Spectral decomposition of the total noise with and without inflow grid

7. OPTIMIZATION APPROACHES CONCERNING THE BROADBAND INSTALLATION NOISE

In this section, some results concerning optimisation approaches with respect to broadband installation noise are briefly given in Tab. 1. The measures, located at the impeller blades, aim at reducing the emitted sound power when flow inhomogeneities as vortices collide with the blades. So in principle, they are also suitable to reduce tonal noise, but in practise, the effectiveness is more given for smaller vortical structures and thus higher frequencies where broadband noise dominates.

Table 1. Investigates measures at impeller blades to reduce sound emissions.

Description	Photograph	Best Results
Slotted Leading edge region		Tonality +-0 dB Broadband -1 dB(A) Efficiency -1%
Porous leading Edge Region		Tonality +-0 dB Broadband +2 dB(A) Efficiency -1%

8. CONCLUSIONS

An investigation of the aeroacoustic installation noise of an evaporator fan in a 12-kW air-to-water heat pump, featuring an L-shaped heat exchanger, is presented in the present work. While modern axial fans often exhibit low self-noise in standardised laboratory conditions, significantly higher noise levels can be observed once integrated into the system. The analysis revealed that the installation noise—arising from the upstream flow conditions—can exceed the fan's self-noise and substantially contribute to the perceived tonality of the emitted sound.

A combination of experimental and numerical methods, including Lattice-Boltzmann simulations and measurements in a certified anechoic facility, enabled a decomposition of self-noise and installation noise. The spectral analysis confirmed that tonal components are amplified due to asymmetric and broadband components due to turbulent inflow, both being strongly influenced by the geometric integration of the fan within the heat exchanger housing.

Three optimisation strategies were tested to reduce tonal components of installation noise: (1) optimised fan positioning, (2) flow-guiding elements, and (3) inflow grids. Among these, shifting the fan towards the short branch of the L-shaped evaporator yielded the most significant acoustic improvement, effectively eliminating tonal penalties without increasing the overall sound power level. While flow-guiding elements and inflow grids showed some positive effects, their performance was highly case-dependent and, in the case of the inflow grid, introduced additional high-frequency noise.

The findings highlight that system-level integration and spatial arrangement of components play a critical role in the aeroacoustic performance of heat pump fans. Future work should focus on the automated optimisation of inflow conditions using simulation-driven design and on establishing robust guidelines for low-noise fan integration in compact heat pump units.

9. ACKNOWLEDGMENTS

This work has been supported by the Federal Ministry for Economic Affairs and Energy (BMWi) in the frame of the collaborative Project “WarmHome” [1].

10. REFERENCES

[1] Collaborative Project “WarmHome”, Grant Number (“Förderkennzeichen”) 03EN4065E, funded by the Federal Ministry for Economic Affairs and Energy (BMWi), Weblink: EnArgus

[2] T. Zhu, and T.H. Carolus: “Axial fan tip clearance noise: Experiments, Lattice–Boltzmann simulations, and mitigation measures”, *Int. J. of Aeroacoustics*, vol. 17.1-2, pp. 159–183, 2018.

[3] F. Lörcher, S. Hub, S. Moreau and M. Sanjosé: “Investigations concerning the flow stabilization of backward curved centrifugal impellers at low flow rate”, *Int. J. of Turbomachinery, Propulsion and Power*, vol. 7(4), 37, 2022, **https://doi.org/10.3390/ijtpp7040037**.

[4] F. Lörcher, “CFD-Based Fan Optimizations considering the System Integration in a Heat Pump”, in *Proc. of Fan 2015 Conf., (Lyon, France)*, 2015.

[5] S. Becker and F. Czwielong: Funding project “Installationseffekte Axial*”*, Grant Number (“Förderkennzeichen”) IGF 20659 N Abschlussbericht (final report), Funded by the BMWi, 2023.

[6] Commercial Reference Fan of size 630 mm *FPowlet-FP063-6IA.BD.V3P1*, manufacturer ZIEHL-ABEGG SE, weblink: Detail - FPowlet - FP063-6IA.BD.V3P1

[7] ISO 5801:2017, “*Industrial Fans: Performance Testing Using Standardised Airways*.”, 2017

[8] S. Chen and G. D. Doolen: *Annual Review of Fluid mechanics* 30:329-364 ISSN 00664189, 1545-4479, 1998.

[9] S. Marié: *Etude de la méthode Boltzmann sur Réseau pour les simulations en aéroacoustique*, Ph.D. thesis Université Pierre et Marie Curie – Paris VI, 2008.

[10] H. Chen, O. Filippova, J. Hoch, K. Molvig, R. Shock, C. Teixeira and R. Zhang: *Physica A: Statistical Mechanics and its Applications*, 362:158-167 ISSN 03784371, 2006.

[11] F. Pérot, M.S. Kim, S. Moreau, M. Henner and D. Neal, “Direct Aeroacoustics Prediction of a Low-Speed Axial Fan”, in *Proc. of 16th AIAA/CEAS Aeroacoustics Conf. (Stockholm, Sweden)*, 2010.

[12] E. Fares: – *Computers and Fluids* 35: 940-950 ISSN 00457930, 2006.

[13] DIN45681:2005-04,“*Acoustics-Determination of tonal components of noise and determination of a tone adjustment for the assessment of noise emissions*.”, 2005